



HAL
open science

Can broad-band earthquake site responses be predicted by the ambient noise spectral ratio? Insight from observations at two sedimentary basins

Vincent Perron, Céline Gélis, Bérénice Froment, Fabrice Hollender, Pierre-Yves Bard, Giovanna Cultrera, Edward Marc Cushing

► To cite this version:

Vincent Perron, Céline Gélis, Bérénice Froment, Fabrice Hollender, Pierre-Yves Bard, et al.. Can broad-band earthquake site responses be predicted by the ambient noise spectral ratio? Insight from observations at two sedimentary basins. *Geophysical Journal International*, 2018, 215 (2), pp.1442-1454. 10.1093/gji/ggy355 . hal-01989182

HAL Id: hal-01989182

<https://hal.science/hal-01989182>

Submitted on 15 Oct 2021

HAL is a multi-disciplinary open access archive for the deposit and dissemination of scientific research documents, whether they are published or not. The documents may come from teaching and research institutions in France or abroad, or from public or private research centers.

L'archive ouverte pluridisciplinaire **HAL**, est destinée au dépôt et à la diffusion de documents scientifiques de niveau recherche, publiés ou non, émanant des établissements d'enseignement et de recherche français ou étrangers, des laboratoires publics ou privés.



Distributed under a Creative Commons Attribution 4.0 International License

Can broad-band earthquake site responses be predicted by the ambient noise spectral ratio? Insight from observations at two sedimentary basins

Vincent Perron,^{1,2,3,*} Céline Gélis,² Bérénice Froment,² Fabrice Hollender,^{1,3}
 Pierre-Yves Bard,³ Giovanna Cultrera⁴ and Edward Marc Cushing²

¹CEA, DEN, F-13108 Saint-Paul-lez-Durance, France. E-mail: vincent.perron.mail@gmail.com

²IRSN, PSE-ENV/SCAN/BERSIN, BP 17, F-92262 Fontenay-aux-Roses, France

³University of Grenoble Alpes, ISTERre, CNRS, IRD, IFSTTAR, F-38000 Grenoble, France

⁴Istituto Nazionale di Geofisica e Vulcanologia, Roma, Italy

Accepted 2018 August 22. Received 2018 August 21; in original form 2018 March 28

SUMMARY

Site-effect assessments performed through earthquake-based approaches, such as the standard spectral ratio (SSR), require good quality records of numerous earthquakes. In contrast, the use of ambient noise appears to be an attractive solution for ease and rapid computation of site responses with sufficient spatial resolution (microzonation), especially in low seismicity areas. Two main approaches are tested here: the horizontal-to-vertical spectral ratio (HVSr) and the noise-based SSR (SSR_n). The HVSr uses the relative amplitude of the horizontal and vertical components of the ambient noise. Instead, the SSR_n defines the spectral ratio between the seismic noise recorded simultaneously at a site and at a rock reference station, similar to earthquake-based SSR. While the HVSr is currently used in hundreds of site-specific studies, the SSR_n approach has been gradually abandoned since the 1990s. In this study, we compare the results obtain from these two approaches with those of earthquake-based SSR. This comparison is carried out for two sedimentary basins, in Provence (southeastern France) and in Argostoli (western Greece). In agreement with the literature, the HVSr does not provide more than the fundamental resonance frequency of the site (f_0). The SSR_n leads to overestimation of the SSR amplification factors for frequencies higher than the minimal f_0 of the basin ($f_{0\min}$). This discrepancy between SSR_n and SSR is discussed, and appears to be mainly dependent on the local geological configuration. We thus introduce the hybrid standard spectral ratio (SSR_h) approach, which aims to improve upon the SSR_n by adding an intermediate station inside the basin for which the SSR is known. This station is used in turn as a local reference inside the basin for the SSR_n computation. The SSR_h provides site transfer functions very similar to those of the SSR, in a broad frequency range. Based on these results, the SSR_n (or SSR_h) should be further tested and should receive renewed attention for microzonation inside sedimentary basins.

Key words: Earthquake ground motions; Site effects; Seismic noise; Body waves; Fourier analysis; Spectral ratio.

INTRODUCTION

Since the first understanding that seismic signals can be locally modified by the geological conditions of the Earth surface (e.g. Milne 1908), it has been widely demonstrated that site effects can dramatically increase both the amplitude and duration of ground

motion. This is a source of particular concern for seismic hazard assessment, as site effects can greatly increase hazard levels in many cities that are located on sedimentary basins (e.g. Mexico City, Mexico; Los Angeles, USA; Tokyo, Japan; Grenoble, France; among others). For example, during the Guerrero-Michoacan event of 1985, ground motions in the basin of Mexico City showed significantly higher amplitudes and duration than in the surrounding rock (Celebi *et al.* 1987), as also more recently during the 2017

* Now at: Swiss Seismological Service (SED), ETH Zürich, Sonneggstrasse 5 CH-8092 Zürich, Switzerland.

M_w 8.1 Chiapas and M_w 7.1 Tehuantepec shocks. After the devastating Guerrero-Michoacan earthquake, the contributions of local site conditions to ground motion became recognized as essential and received particular attention. Since then, increasing numbers of studies have tried to assess site effects from what is sometimes called the ‘ambient seismic field’, and is here (albeit incorrectly) referred to as ‘ambient noise’, for brevity. However, the advantage of using ambient noise has long since been recognized (e.g. Ishimoto 1937). Indeed, ambient noise can be recorded everywhere at any time, which makes its use fast, easy and inexpensive when compared to earthquake data processing. Assessing seismic site responses from ambient noise is thus of major interest to locally infer the spatial variations of site effects (i.e. microzonation), especially in low-to-moderate seismicity areas.

The ground motion (U) at a given position can be seen as convolution in the time domain (or multiplication in the frequency domain) between a source (S), a path (P) and a site (H) term:

$$U(f) = S(f) \times P(f) \times H(f), \quad (1)$$

where f is the frequency. The so-called site transfer function, $H(f)$, gives the amplification factor relative to a reference position for each frequency. The most common and reliable way to assess this is the standard spectral ratio (SSR) technique (Borcherdt 1970; see also e.g. Field & Jacob 1995; Bonilla *et al.* 1997). This approach relies on the simultaneous records of the same earthquake for at least two stations that are close enough with respect to the earthquake distance. In practice, the station located under the best possible geological conditions is used as the reference (i.e. with minimum site amplification; generally a rock site). The transfer functions are obtained by normalizing the Fourier amplitude spectrum (FAS) of ground motions recorded at the site under study according to the FAS recorded at the reference site. The SSR assumes that the incident signal at depth is the same for the site and the reference; that is that both stations ‘see’ the same source and path terms. It is generally accepted that this assumption is true if the hypocentral distance is much greater than the site-to-reference distances. This normalization is used to cancel out the source and path terms of the signal, and can be summarized as follows:

$$SSR_{x/r}(f) = \left\langle \frac{\{|U_x(f)|\}}{\{|U_r(f)|\}} \right\rangle_{\log}, \quad (2)$$

where $SSR_{x/r}$ is the SSR between a site s_x and the reference site s_r (see Fig. 1). For each component, $|U_x(f)|$ and $|U_r(f)|$ are the FAS evaluated from the earthquake signals at sites s_x and s_r , respectively. The curly brackets $\{\cdot\}$ represent spectral smoothing, and the arrowhead brackets as $\langle \cdot \rangle_{\log}$ represent the geometric (logarithmic) mean over the earthquake recordings.

To be applicable, however, this technique requires many earthquakes to be recorded at both stations, with good signal-to-noise ratio in a wide frequency band (e.g. Perron *et al.* 2015). Such a good quality dataset is not always available, as this depends on the instrumental network deployment, the seismotectonic environment, and the local noise perturbation. For sites where such an approach is not possible, techniques based on ambient noise appear to be an appealing alternative.

The use of ambient noise for site response assessment presents some limitations, as the location of noise sources and the wavefield content are generally not known and differ from earthquakes, such that: (i) the response of sediments to ambient noise generated and propagating mainly at the surface has to be related to that of the incident seismic waves from earthquakes; (ii) the source and path

terms of the ambient seismic field have to be canceled out when computing the spectral ratio, to isolate the site influence. For the first limitation, several studies showed that ambient noise is mainly dominated by surface waves, as the sources are almost entirely located at the Earth surface (e.g. atmospheric phenomena, human activities) (e.g. Bonnefoy-Claudet *et al.* 2006b). On the contrary, the earthquake signal is mainly composed of body waves in strong-phase motion. For the second limitation, isolation of the site term is not obvious, because, as opposed to earthquake signals, a deterministic description is not appropriate for the random seismic noise generated by various sources. However, different approaches have been developed generally over the last three decades to extract some information related to site responses from the amplitude of ambient noise recordings. Among these, the most usual approach is the horizontal-to-vertical spectral ratio (HVSr), which is used in practice to assess the spatial variability of the fundamental resonance frequency (f_0) of a site. The ambient noise SSR (SSRn) attempts to assess the site transfer function by simultaneously normalizing the noise recorded at a site according to that recorded at a rock reference station, in a similar way to the SSR approach from earthquake recordings. A short review of these methods is given in the next section, with particular attention to the SSRn approach. For more detailed reviews, the reader is invited to refer to the following studies: Field *et al.* (1990) provides a good overview of the preliminary approach used to characterize site responses from ambient noise, and includes the first studies on the SSRn; in the same way, Lermo & Chávez-García (1994), Kudo (1995) and Bard (1999) provide comprehensive reviews of the initial development and applications of the SSRn and HVSr approaches; and Bonnefoy-Claudet *et al.* (2006b) provides the literature on the HVSr in detail.

While the HVSr cannot be used to assess the site transfer function, $H(f)$, at any frequency, the SSRn has been primarily used in the low frequency range (<1 Hz, see ‘Methods definition and background’ section). At these frequencies, ambient noise is indeed dominated by coherent Rayleigh waves that are generated by known and generally distant oceanic sources (microseisms). At higher frequencies (>1 Hz), ambient noise is mainly composed of Love and Rayleigh waves; it is also more complex and is dominated by human activities (microtremors). Site effects are rarely negligible above 1 Hz, even for deep basins where higher resonance modes, 2-D/3-D effects, and shallow velocity contrast can notably amplify the short wavelengths. Evaluation of $H(f)$ for frequencies >1 Hz is essential, as this is the frequency range that is classically targeted in engineering applications (1–10 Hz). Moreover, geological and geophysical models used in numerical simulations do not yet have sufficient resolution to predict ground motion up to high frequencies, which makes empirical approaches the only available way to assess site responses up to these frequencies. Using microtremors is thus primordial, but challenging, due to their more difficultly predictable nature and origin. As the frequency range we are working on in this study is predominately >1 Hz, the terms ‘microtremors’ and ‘ambient noise’ are used indiscriminately in the following.

The aim of this study is to experimentally estimate the use of noise-based spectral ratio approaches to assess site transfer functions calculated for weak motion earthquake solicitations, up to high frequencies. Here, we develop a new approach, the hybrid SSR (SSRh), to assess the spatial variability of site responses from a temporary network placed around a permanent or long-term recording station for which an SSR transfer function is already available. We benefit from datasets that were acquired on two different sites: an industrial site located across a small sedimentary basin in the low-to-moderate seismicity context of Provence (southeastern France);

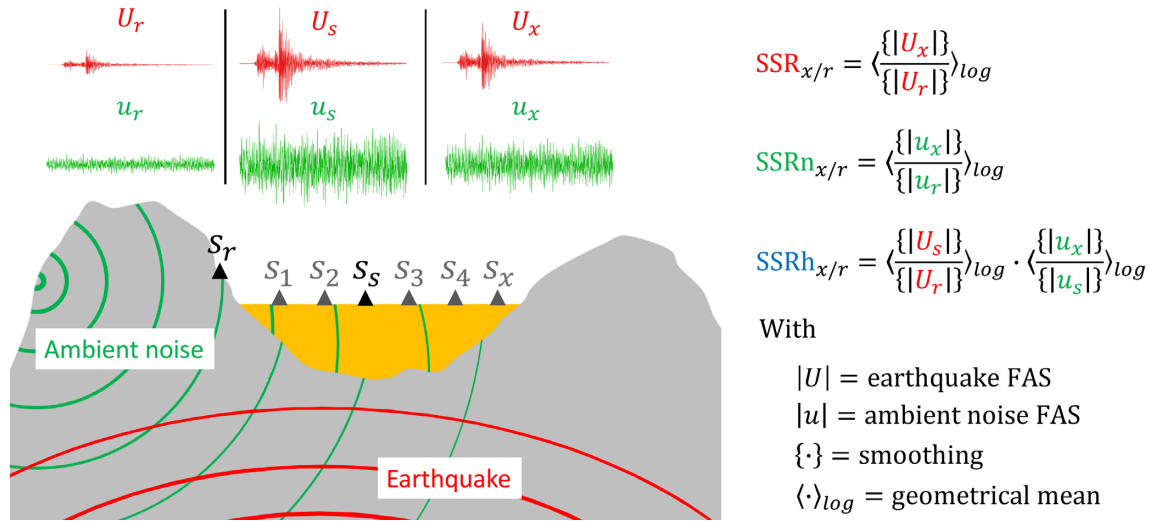


Figure 1. Illustration of the SSR, the SSRn, and the SSRh methods for the case of a sedimentary basin. The two permanent stations (s_r and s_s) are presented in black, while the temporary network (from s_1 to s_x) is represented in gray. FAS, Fourier amplitude spectrum.

and a sedimentary basin located close to the town of Argostoli, on the seismically active island of Cephalonia (western Greece). We compare the results obtained from spectral ratio approaches using noise recordings (i.e. HVSR, SSRn, SSRh) with those obtained from weak motion recordings (SSR), taken here as the reference results. Finally, we discuss the dependence of our results on local geological configurations, and propose a qualitative interpretation for the widely observed SSRn overestimation at high frequencies.

METHODS DEFINITION AND BACKGROUND

Horizontal-to-vertical spectral ratio

The HVSR approach consists of computing the spectral ratios between the horizontal mean component and the vertical components of microtremors recorded simultaneously at one single station. This can be written as:

$$HVSR_x(f) = \left\langle \frac{\{|u_{xH}(f)\}}{\{|u_{xV}(f)\}} \right\rangle_{\log}, \quad (3)$$

where $HVSR_x$ is the HVSR at site s_x , and $|u_{xH}(f)|$ and $|u_{xV}(f)|$ are the FAS evaluated from ambient noise recorded at site s_x for the mean horizontal and vertical components, respectively. This approach was first introduced in Japan in the 1970s (e.g. Nogoshi & Igarashi 1971). At the end of the 1980s, Nakamura (1989) proposed its first versions in English, which led to this technique being called Nakamura's method. Later on, Kudo (1995) and others popularized its use. Nakamura (1989) interpreted the HVSR curves as the amplification of the site due to S -wave resonance. However, it is currently acknowledged that the HVSR allows for estimation of only f_0 of S waves propagating in 1-D sites, mainly due to the surface waves present in ambient noise. Indeed, the ellipticity of the Rayleigh waves results in the vanishing of the amplitude of the vertical components at f_0 , while the Airy phase of Love waves leads to a bump of energy on the horizontal components at f_0 . Both of these phenomena result in a peak in the H/V ratio close to f_0 . The reliability of this technique to assess f_0 for simple 1-D geological structures with strong impedance contrast has been demonstrated both theoretically and experimentally (see Bonnefoy-Claudet *et al.*

2006a). As the HVSR provides a fast, easy and low-cost solution for f_0 microzonation, the number of studies based on this approach has dramatically increased over the last three decades. A comprehensive review of the HVSR is thus not possible here. A long debate has continued on the use of the HVSR to assess the amplification factor of site responses. Indeed, a project that faced this topic led to implementation of extensive HVSR recommendations (SESAME team 2004; http://sesame.geopsy.org/Delivrables/Del-D23-HV_User_Guidelines.pdf). Following this recommendation, the HVSR approach was shown not to be reliable to infer resonance frequencies at higher modes (i.e. above f_0), and the amplification factor at any frequency. Nevertheless, some recent applied and theoretical research on the HVSR investigated the possibility to exploit more than just the main peak frequency of the HVSR to provide additional information on seismic amplification effects and elastic properties of shallow geologic structures (e.g. Sánchez-Sesma *et al.* 2011; Kawase *et al.* 2015; Piña-Flores *et al.* 2017).

Noise-based standard spectral ratio

In the 1980s, a decade after the first definition of the SSR approach by Borchardt (1970), the SSRn was introduced (Irikura & Kawanaka 1980; Kagami *et al.* 1982, 1986). This is equivalent to the SSR (eq. 2) but is applied to ambient noise:

$$SSRn_{x/r}(f) = \left\langle \frac{\{|u_x(f)\}}{\{|u_r(f)\}} \right\rangle_{\log}, \quad (4)$$

where $SSRn_{x/r}$ is the SSRn between a site s_x and the reference site s_r (see Fig. 1), and $|u_x(f)|$ and $|u_r(f)|$ are the FAS evaluated from ambient noise at each component at sites s_x and s_r , respectively. One important preliminary condition for using the SSR and SSRn techniques to assess sedimentary site responses is the availability of a nearby rock reference site, where the site response can be considered as negligible. Studies based on microseisms (<1 Hz) generally rely on distant oceanic sources. However, as the ambient noise period decreases, its dependence on local sources increases (e.g. Aki 1988). At higher frequencies (>1 Hz), proximity of the microtremor sources is then expected. This clear difference in terms of minimal

distance to the source required for the SSR creates further difficulties when microtremors are used to estimate site transfer functions that are comparable to those provided by earthquake-based SSR.

The SSRn has been tested in several studies, to either detect the presence of a fault at depth (e.g. Irikura & Kawanaka 1980) or to assess site responses. The first evaluation for site effect purposes was that of Kagami *et al.* (1982, 1986) at low frequencies (0.1–1 Hz). Since this evaluation, numerous studies have applied the SSRn under different experimental conditions (for an extended review, see Perron 2017). Some studies only made qualitative comparisons of the SSRn with the geology of the sites (Kagami *et al.* 1982, 1986; Okada *et al.* 1991; Ferritto 1995; Koyama *et al.* 1996; Milana *et al.* 1996; Haile *et al.* 1997; Ibs-von Seht & Wohlenberg 1999; Burjánek *et al.* 2012; Hashemi & Maazallahi 2012) and/or with the degree of damage after major earthquakes (Ohmachi *et al.* 1991; Koyama *et al.* 1996; Haile *et al.* 1997; Seo *et al.* 2000). Several other studies obtained mixed results for comparisons between SSR (or sometimes theoretical site transfer functions) and SSRn curves, which depended mainly on the experimental conditions (e.g. type of soil, level and proximity of noise sources, distance between stations and reference site) and on the processing (e.g. instrument used, criteria for selection of noise windows, stacking, frequency bands evaluated). Some of these obtained at least rough estimates of the site transfer functions using the SSRn approach, generally at low frequencies (Rovelli *et al.* 1991; Gutierrez & Singh 1992; Yamanaka *et al.* 1993; Lermo & Chávez-García 1994; Gitterman *et al.* 1996; Zhao *et al.* 1998; Horike *et al.* 2001; Steimen *et al.* 2003; Roten *et al.* 2006; Theodoulidis 2006). Some studies succeeded in achieving only f_0 (Celebi *et al.* 1987; Field *et al.* 1990; Gaull *et al.* 1995; Seekins *et al.* 1996; Atakan 1997), while a few others did not find any convincing agreement between SSRn and SSR (Seo 1992; Field *et al.* 1995; Field 1996). The majority of these studies concluded that the SSRn method is reliable to predict at least, f_0 , but cannot be used to estimate the amplification factors of site responses over the whole frequency band. They often observed unrealistically high amplification factors at high frequencies that they hypothesized to be due to local noise source disturbance that masked the site effects. In a different way, Dravinski *et al.* (1996) theoretically investigated the potential of the HVSR and the SSRn to assess the responses of a semicircular and semi-spherical valley to incident plane harmonic Rayleigh waves. They reported better estimations of resonance frequencies (f_0 , and higher modes) and amplification with the SSRn, than with the HVSR.

As the SSRn method provided mixed results on the site response assessment, and because of the ramp up of the HVSR method, the SSRn was gradually abandoned. However, only a few studies specifically paid attention to the origin and distribution of the noise sources, the site-to-reference distance, and/or the geological configuration of the surrounding area. Horike *et al.* (2001) tested the SSRn on a large array (diameter, 5 km) and a small array (diameter, 0.5 km) between 1 and 10 Hz. The small array was located on a volcanic ash terrace, as was the reference, while the majority of stations of the large array were located on a sand plain. They reported that SSRn provided reliable amplification factor of up to 5–8 Hz for the smaller area. For the larger area, they did not succeed in finding the amplitude, even if the general shape of the SSRn transfer function was relatively similar to those from the SSR. They again explained this discrepancy by the probable presence of close anthropic sources, and concluded that the incoming microtremors were the same only within limited areas of a few hundreds of metres in diameter. However, they did not discuss possible influences of the differences in geological conditions between the two areas.

Hybrid standard spectral ratio

We introduce here the SSRh approach that combines the SSRn based on ambient noise recording with the classical SSR computed from earthquake recordings. The SSR is used to assess the rock relative site response at one location inside the basin, and thus requires only two long-term or permanent stations. Then, the spatial variability of the basin response (microzonation) is estimated through the SSRn computed using several short-term recording stations inside the basin, and is relative to the soil station for which the rock relative SSR transfer function is known. The SSRh can be expressed as:

$$SSRh_{x/r}(f) = SSR_{s/r}(f) \cdot SSRn_{x/s}(f), \quad (5)$$

where $SSRh_{x/r}$ is the SSRh at site s_x relative to the rock reference site s_r , $SSRn_{x/s}$ is the SSRn evaluated at site s_x relative to the soil reference site s_s , and $SSR_{s/r}$ is the classical SSR at s_s relative to s_r (see Fig. 1).

Eqs (2), (4) and (5) finally give:

$$SSRh_{x/r}(f) = \left\langle \frac{|U_s(f)|}{|U_r(f)|} \right\rangle_{\log} \cdot \left\langle \frac{|u_x(f)|}{|u_s(f)|} \right\rangle_{\log}, \quad (6)$$

where $|U_s(f)|$ and $|u_s(f)|$ are the FAS evaluated at the soil reference site s_s from the earthquake signal and from ambient noise, respectively. The main idea behind the SSRh is to ensure that the SSRn reference site is closer to the studied sites and under the same geological conditions (i.e. inside the basin). The SSRh approach aims to capture the site response spatial variability inside the sedimentary basin from microtremors. Ferritto (1996) initially suggested the use of a reference site inside the basin, whereby he assessed the SSRn relatively to a soil reference station co-located with a borehole where boring logs had been kept. He used the SSRn to describe the spatial variability of the site response, and he proposed to use the borehole information to deduce the rock relative site response. He observed good stability of the general shape of the relative transfer functions, and concluded that the SSRn referred to soil sites is a good tool for microzonation.

DATA AND PROCESSING

Provence site array

This studied industrial area is located in Provence in the south-western Alpine foreland (southeastern France). This region is seismically relatively active compared to other regions of mainland France, even though the seismic activity of this area remains low-to-moderate (e.g. Manchuel *et al.* 2017). Fig. 2 presents the geological map and the locations of the stations used in this study. Stations P1 and P2 are located on outcropping massive Cretaceous limestone. Stations P3–P7 are located within a relatively small paleo-valley (a few hundred metres wide, 50–150 m deep) filled with stiff Miocene sands/sandstone, and softer Quaternary deposits. Based on geophysical measurements, the time-averaged shear-wave velocities within the first 30 m of soil (V_{S30}) are evaluated as 2100, 1800, 440 and 720 m s⁻¹ from P1 to P4, respectively (Perron *et al.* 2017a). According to the National Earthquake Hazards Reduction Program classification, sites P1 and P2 thus belong to the ‘hard rock’ class, while sites P3 and P4 belong to the ‘very dense soil’ class. The velocity profiles measured at the rock site P1 and the soil site P4 using two invasive techniques (crosshole and PS Suspension Logging) are shown in Fig. 2. Site P1 was also investigated with seismic noninvasive techniques, as it was one of the studied sites in

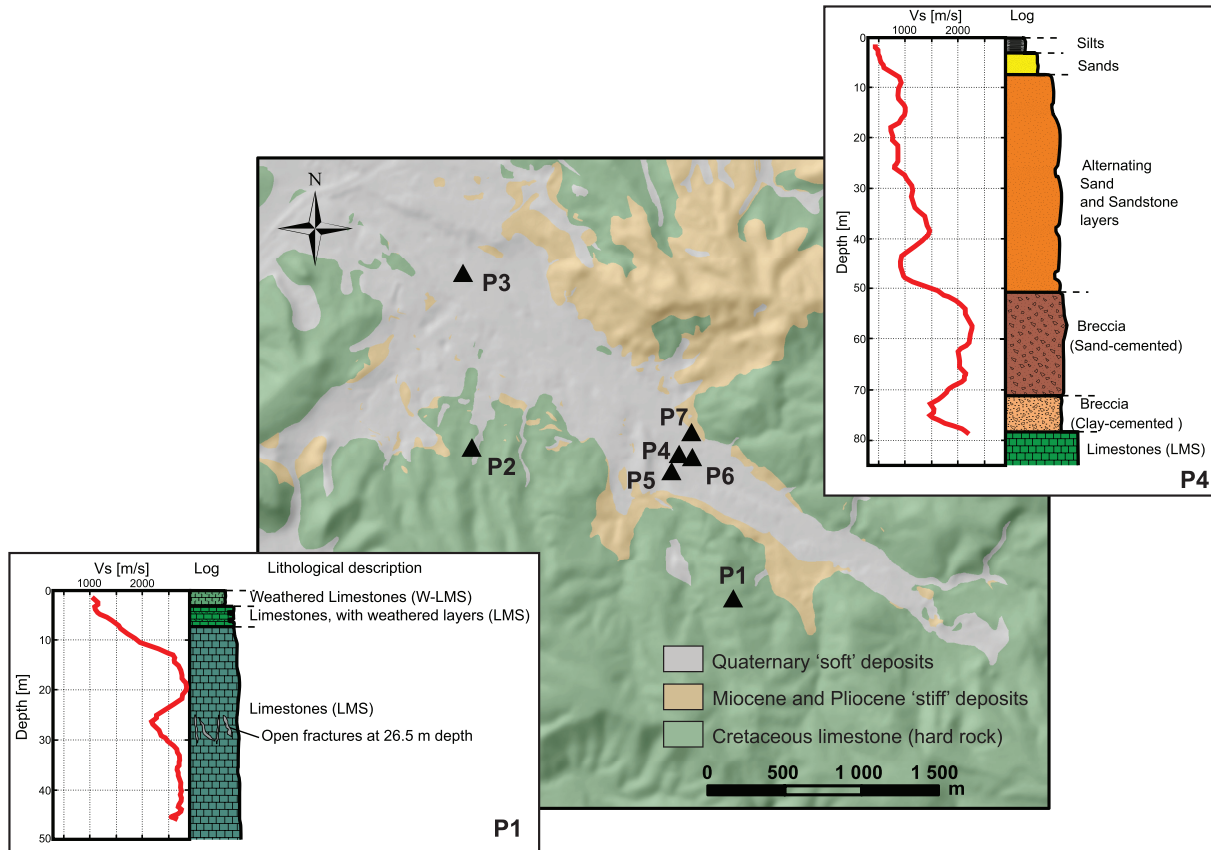


Figure 2. Geological map of the recording area in Provence. P1 and P2 are the rock sites, and P3–P7 are the five stiff soil sites. At stations P1 and P4, three boreholes allowed for determination of the shear-wave velocity profile with depth [$V_S(z)$] from two different techniques: crosshole and PS Suspension Logging.

the interPACIFIC project (Garofalo *et al.* 2016). The sensors were Güralp CMG6-TD broad-band velocimeters with a sampling rate of 100 Hz. They were continuously recording for from a few months to more than 2 yr, depending on the station (Perron *et al.* 2015). The main database is composed of data recorded continuously between February 2012 and June 2014 at all sites. More than 500 weak motion earthquakes were recorded, which were mainly low magnitude regional earthquakes (M_L from 1 to 2.5).

Argostoli array

Cephalonia Island (western Greece, Ionian Island) is located at the northwestern end of the Aegean subduction frontal thrust, which is linked to the dextral Cephalonia-Levkas transform fault to the west of Cephalonia. The seismotectonic context is one of the most active in Europe, and destructive earthquakes can occur in this area, such as the 1953 $M7.3$ earthquake. The Plio-Quaternary and Pliocene Koutavos basin is located on a NW-striking syncline bounded to the west by a thrust asymmetric anticline (Fig. 3). The western flank of this anticline is faulted by two east-dipping active reverse faults (i.e. White Rock Fault, Argostoli Fault).

A high resolution experiment took place from September 2011 to April 2012 in the framework of the FP7 EU-NERA 2010–2014 project (Network of European Research Infrastructures for Earthquake Risk Assessment and Mitigation, https://cordis.europa.eu/project/rcn/96282_en.html; Theodoulidis *et al.* 2018). This experi-

ment was conducted by four institutes (*Institut des Sciences de la Terre* [ISTERRE], Grenoble, France; *Instituto Nazionale di Geofisica e Vulcanologia* [INGV], Rome, Italy; *GeoForschungsZentrum* [GFZ], Potsdam, Germany; Institute of Engineering Seismology and Earthquake Engineering [ITSAK], Pilea Chortiatis, Greece) and the continuous recorded data are available through the European Integrated Data Archive (network code 4C in www.orfeus-eu.org/eida/). Hereafter, we present results obtained from a limited part of this network, named here from N1 to N11 and which corresponds to the 11 velocimeters installed by INGV (KER02, KES02, KES04, KES06, KES08, KES11, KES13, KES14, KES16, KES18, and KES22 in Theodoulidis *et al.* 2018). All of these velocimeters were Lennartz 5 s with 100 Hz sampling rate. This subarray was roughly aligned along a profile across the sedimentary basin, as shown in Fig. 3. N1 is the rock reference site while N6 was chosen as the sedimentary reference site. Hundreds of regional weak motion earthquakes have been recorded (Cultrera *et al.* 2014). The shear-wave velocity profile at the centre of the sedimentary basin is given in Fig. 3. Both the geological map and the velocity profile were determined afterwards, by the Sinaps@ project (<http://www.institut-seism.fr/projets/sinaps/>). The ‘Argonet’ permanent vertical network was installed in 2015 at the surface and the depth of the borehole, and was used together with ambient noise array measurements to determine the velocity profile (Hollender *et al.* 2015; Cushing *et al.* 2016; Perron *et al.* 2018).

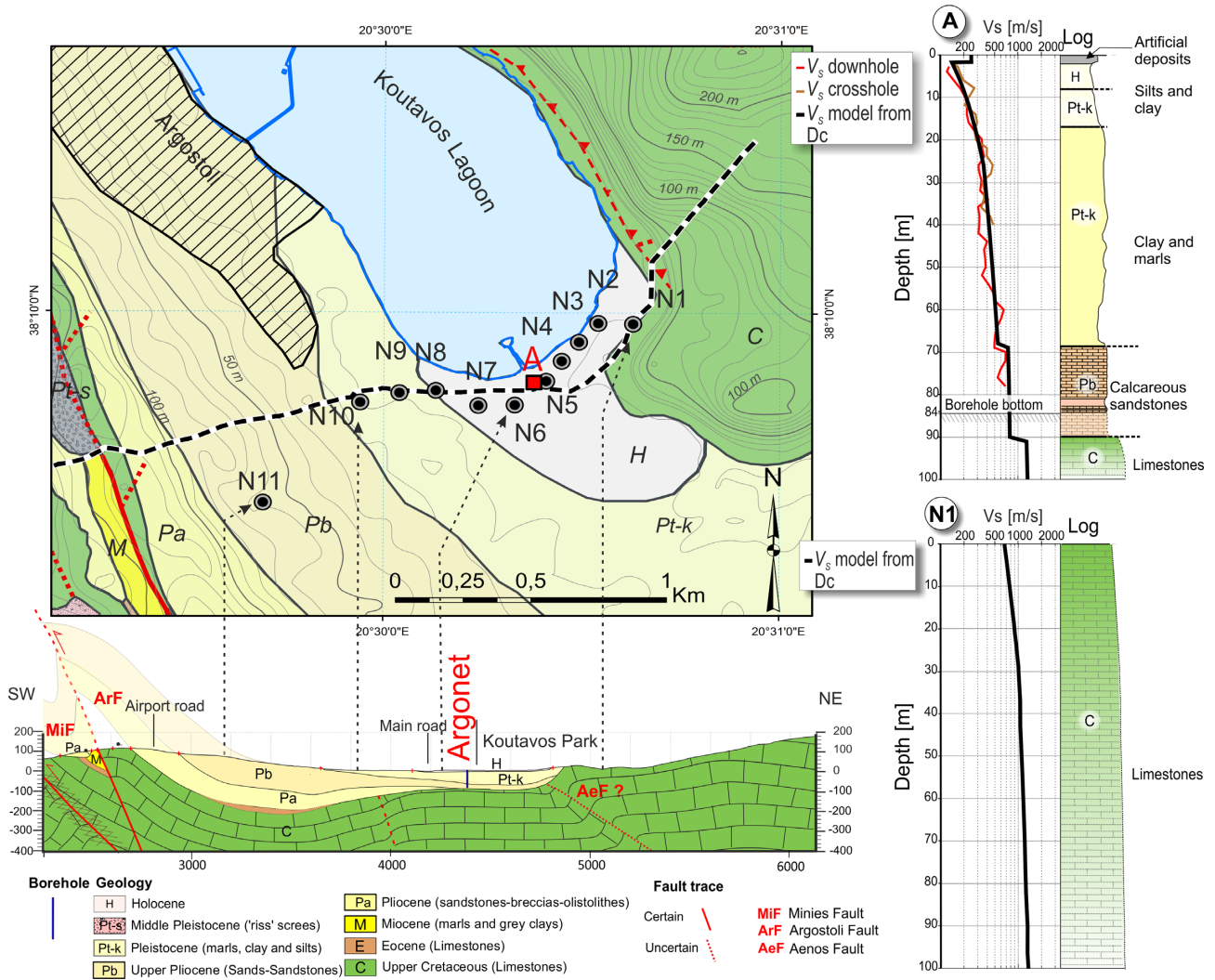


Figure 3. Geological map and section of the recording area near Argostoli. N1 is the reference rock site located on limestone, while N2 to N11 are the soil sites across the basin. At site A (red square) three boreholes allowed for determination of the shear-wave velocity profile with depth [Vs(z)—top right] from two invasive techniques: crosshole and downhole. A temporary network at the surface also gave the opportunity to assess the velocity profile from the surface waves dispersion curve inversion at sites N1 (bottom right) and A.

Processing

Classical earthquakes processing was used to compute the SSR. In Provence, the FAS of the SSR in eq. (2) were processed from the entire signal of tens to hundreds of weak motion earthquakes, depending on the site. The SSR were estimated also from the P waves, S waves and coda waves alone, leading to similar results (an example is given later, in Fig. 6). The windowing procedure proposed by (Perron *et al.* 2017b) was followed to select different parts of the signal. The full signals are detrend and a 5 per cent cosine taper is applied to the edge of the signal window. For each frequency, the geometric mean is estimated from earthquake spectrum parts that satisfy a signal-to-noise ratio >3. In Argostoli, the SSR curves used here are those that were computed by Theodoulidis *et al.* (2018), in a similar way.

Processing choices have been poorly discussed when dealing with the amplitude of ambient noise, especially for the SSRn approach. While guidelines were suggested by the SESAME team (2004) to compute the HVSR, the ambient noise processing has been investigated recently in the noise correlation framework mainly focused on

extracting information from the phase of ambient noise (e.g. Bensen *et al.* 2007; Baig *et al.* 2009; Prieto *et al.* 2011; Seats *et al.* 2012; Melo *et al.* 2013; Bowden *et al.* 2015; Yoritomo & Weaver 2016). These studies were aimed at reducing transient noise to improve the emergence of the Green’s function in the correlation functions. Indeed, transient noise might perturb the stationarity of the ambient noise field: at low frequency, transient noise is composed of teleseism events and storms, for example, while at higher frequencies it corresponds principally to anthropic activity (e.g. footsteps, nearby traffic).

Here, the general recommendations derived from the noise correlation community were followed to select the ambient noise time windows that are used to compute the HVSR, SSRn and SSRh curves. In Provence, 150 files of 1 hr of noise were randomly selected from the continuous data after having been through a complete checking process. Each 1-hr file is windowed as 60 windows of 1 min. Each 1-min window (at the site or at the reference) with peaks that exceed 10 times the standard deviation evaluated from the full 1 hr of data are removed, following Denolle *et al.* (2013). If more than 70 per cent of the 1-min windows are removed then the

full 1-hr window is rejected. Otherwise, for each 1-hr window, the average spectrum and associated coefficient of variation are evaluated from the selected 1-min windows. If the average coefficient of variation on the whole frequency band is higher than 100 per cent, or if the maximal coefficient of variation between 0.2 and 15 Hz exceeded 150 per cent, then the full 1 hr is rejected. In Argostoli a similar procedure was followed, although the continuous data were recorded in 24-hr files and the ambient noise level was higher than in Provence, leading to the selection of data for 8 hr at night from 25 daily files. Similar to the Provence dataset, 1-min windows are extracted from each 8-hr record. At the end of the selection process for both sites, thousands of 1-min windows were selected. These selected 1-min windows recorded simultaneously for each component at the site and at the reference site are then used to compute the HVSR, the SSR_n and the SSR_h through eqs (3), (4) and (6), respectively.

The processing of the FAS is identical for both ambient noise and earthquake-based approaches. As the distribution of the results that rely on spectral ratio techniques is log-normal (Perron *et al.* 2015), the geometric mean is considered for each approach. The FAS are smoothed using the Konno & Ohmachi (1998) procedure, with a *b*-value of 30, and resampled on a logarithmic scale. The horizontal mean component is estimated as the quadratic mean of the east–west and north–south component ($\sqrt{(EW^2 + NS^2)/2}$).

COMPARISON BETWEEN SPECTRAL RATIOS FROM MICROTREMORS (HVSR, SSR_n AND SSR_h) AND FROM EARTHQUAKES (SSR)

Figs 4 and 5 show the horizontal mean component of the site transfer functions estimated from the HVSR (brown), the SSR_n (green) and the SSR_h (blue) in comparison with the SSR (red), for the Provence and Argostoli networks, respectively. The rock reference stations are P1 and N1, and the soil reference stations for the SSR_h approach are P4 and N6, for the Provence and Argostoli arrays, respectively. In Provence, taking P2 as rock reference has been tested but is not represented here, as it showed no difference in the observations that could not have been predicted by looking at the SSR and SSR_n between P2 and P1, and because it led to the exact same interpretations as these drawn up with the rock-reference P1. For each station, the distance to the reference (Δd) for both referenced microtremor approaches (i.e. SSR_n, SSR_h) is indicated, as well as f_0 for each site where the HVSR and SSR curves allowed this to be picked (Figs 4 and 5, black dotted lines). f_0 is chosen, where it is possible, as the beginning frequency of the plateau observed for the SSR. This plateau shape is certainly due to lateral variations in the soil properties and to the geometry (i.e. 2-D/3-D effects) of the basins in Provence (e.g. Perron 2017) and in Argostoli (e.g. Imtiaz *et al.* 2017). According to the available SSR and HVSR curves, the lower f_0 (f_{0min}) is approximately 3–4 Hz for the Provence basin, and 1.5 Hz for the Argostoli basin. It is very likely due to the pronounced velocity contrast present at 50 and 90 m deep beneath the Provence and Argostoli basin, respectively. As expected, f_{0min} is obtained for the site that coincides with the deepest parts of the basin for both areas (i.e. P4, P6; N2–N6). For Argostoli, at sites N7–N11, f_0 is less clear, and the amplification factors are lower on average than for sites N2–N6. These observations agree with the complex geological structures of the southwestern part of the basin (Fig. 3), which indicates variations in the thickness of the

superficial layers and stiffer soil conditions (i.e. lower Pleistocene and lower Pliocene).

Horizontal-to-vertical spectral ratio

In agreement with the literature, the HVSR for both of these networks shows a peak at the fundamental resonance frequency (f_0) for some sites (e.g. P4, P6, N4, N5 and N6), which agreed with the SSR curves. These sites correspond predominantly to those located at the centre of each basin, where the lateral variations are smooth. For some sites, the SSR plateau shape also appears to be visible for the HVSR curve, where the first peaks are not sharp (e.g. sites P3, N7–N11). Accurate picking of f_0 can be difficult in cases of broad-band HVSR shape. Whatever the HVSR curve, the resonance frequencies for higher modes (above f_0) are not visible, and the amplification factors are always underestimated for the whole frequency band. Thus, this approach cannot reproduce the site transfer function obtained from the SSR, and can only help to detect f_0 for some sites.

Noise-based standard spectral ratio

Good agreement is observed between the SSR_n and the SSR curves for every site at low frequency, as up to 4 Hz in Provence and 1.5 Hz in Argostoli. These frequencies are stable across all sites and independent of the site-to-reference distance. It can be noted that these frequencies are close to the f_{0min} determined for each basin. For frequencies higher than f_{0min} , the amplitudes of the SSR_n are widely overestimated, even if the general shapes of the transfer functions are roughly similar to the SSR ones. This overestimation of the SSR_n at high frequency has been widely reported in the literature, and is considered further in Section 'Discussion'.

Hybrid standard spectral ratio

The SSR_h site transfer functions are very similar to the SSR up to approximately 10–12 Hz for all of the soil sites in Provence. At higher frequency, very local noise sources may affect differently noise recordings from one station to another leading to discrepancies between SSR_h results and SSR site transfer functions. In the Argostoli basin, good agreement is seen for the full frequency range available (up to 20 Hz) and for most of the sites. Indeed, a slight discrepancy is seen for sites N10 and N11, which are located on stiffer soils than the other sites. As for the SSR_n, the reliability of the SSR_h results, when compared to the SSR, seems independent of the site-to-reference distance (from 87 to 1835 m). The SSR_h approach thus appears to be reliable to predict a large part of the site transfer function (i.e. f_0 and higher resonance modes, and the amplification factor) up to high frequencies. To the best of our knowledge, this is the first time that a microtremor-based approach has accurately reproduced the SSR transfer function over such a broad frequency range.

DISCUSSION

The ambient noise represents an appealing way to predict ground motion in large areas at limited cost and time, especially in low seismicity areas where only few earthquakes can be recorded in several months. It is of major interest to understand what controls the ability, or otherwise, of these microtremors approaches to predict the ground motion that would be induced by an earthquake.

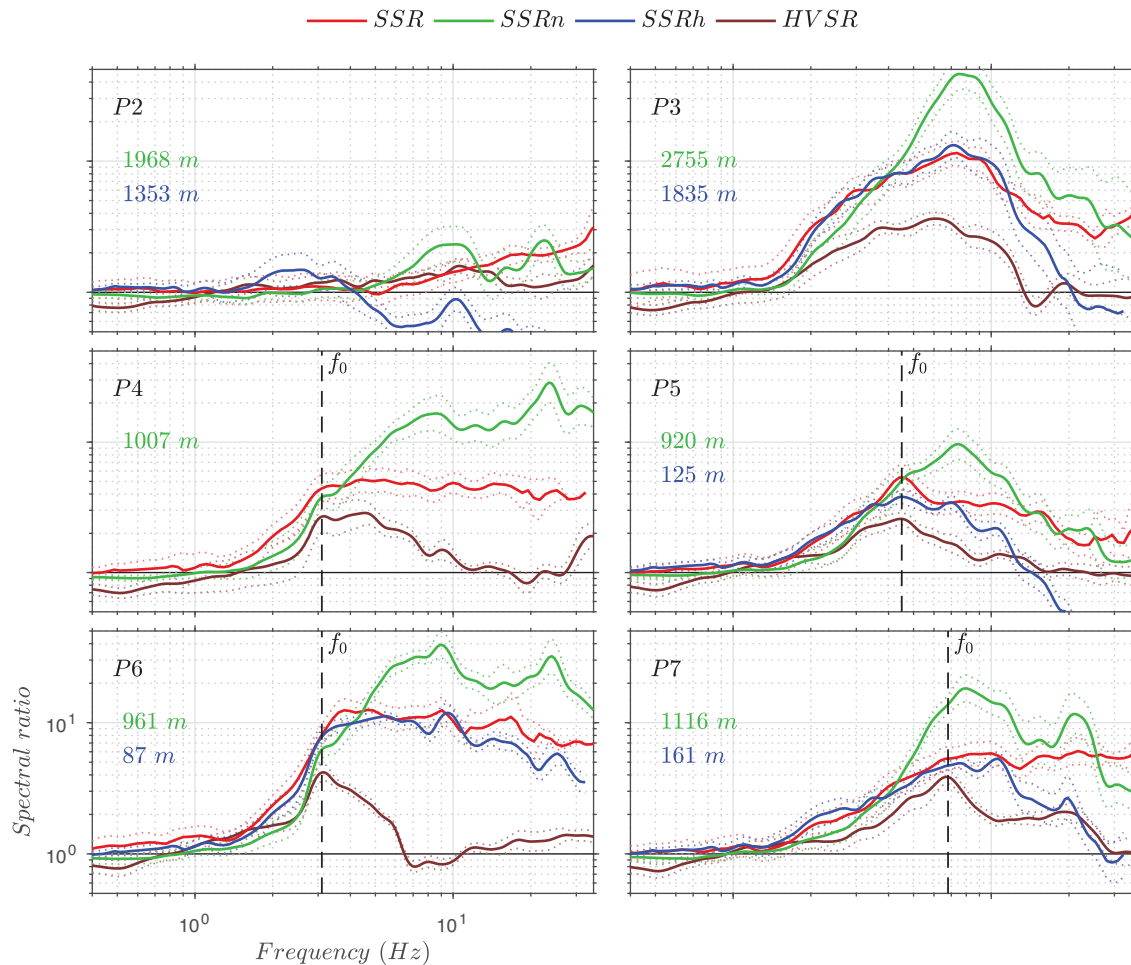


Figure 4. Comparisons of the horizontal mean components of the SSR (red), the SSRn (green), the SSRh (blue) and the HVSR (brown) in Provence at stations P2–P7, with the rock station P1 as reference. P4 is the soil reference used for the SSRh technique. The Δd distances to station P1 (green) and to station P4 (blue) are indicated for each panel, while f_0 (black dashed lines) is given for sites that provide a noticeable peak in the HVSR and/or the SSR. The solid and dotted lines represent the geometric means with their corresponding plus and minus standard deviation computed from more than a hundred earthquakes for the SSR, and from thousands of selected noise windows for the HVSR, the SSRn and the SSRh.

In the following, we discuss two issues to deal with when using microtremors: (i) the response of sediments to ambient noise generated and propagating mainly at the surface has to be related to that of the incident seismic waves from earthquakes and (ii) the source and path terms of the ambient seismic field have to be canceled out when computing the spectral ratio, to isolate the site influence.

On the agreement between microtremors and earthquake-based approaches

The potential for the use of microtremors for evaluation of site effects has long been debated, as body waves emitted by earthquakes are believed to arrive with a quasi-vertical incidence whereas microtremors are mainly composed of surface waves that propagate horizontally. The theoretical point of view is not discussed here, but we address this question through the experimental comparisons between the SSR and the SSRn for two sites located inside the Provence basin. Fig. 6 shows the comparison between the geometric mean of SSRn estimated at site P3 relatively to P4, which are almost 2 km apart, and the geometric mean the SSR computed from various phases of 100 earthquakes (i.e. P wave, S wave, coda wave,

full signal). The relative site responses for the mean horizontal component estimated from ambient noise and from the different phases of the signal are very close up to 12 Hz. This is also the case for the vertical component, even if the discrepancy of the geometric mean of the SSRn above 3 Hz is a little higher. This comparison illustrates why the SSR and SSRh results are so close in Figs 4 and 5, the latter using a SSRn reference station inside the basin (Fig. 1). This confirms the concept that the SSRn can be used to assess responses of a site to weak motion solicitations when both stations are placed inside the basin; that is in the same geological configuration. This occurs despite different wavefield contents and propagation between the earthquake signals and noise.

Few studies have proposed explanations for some of the apparent agreement between spectral ratios from microtremors and from earthquake recordings. Field & Jacob (1993) computed the theoretical responses to ambient noise sources of a horizontally stratified sedimentary layer, and they reported that the expected horizontal component spectrum of ambient noise contains its most prominent peak at the f_0 predicted for incident shear waves. Horike *et al.* (2001) observed good agreement between the SSRn and the SSR for sites located under similar geological conditions. Based on the study of Horike *et al.* (2001) and Satoh *et al.* (2001) explained this

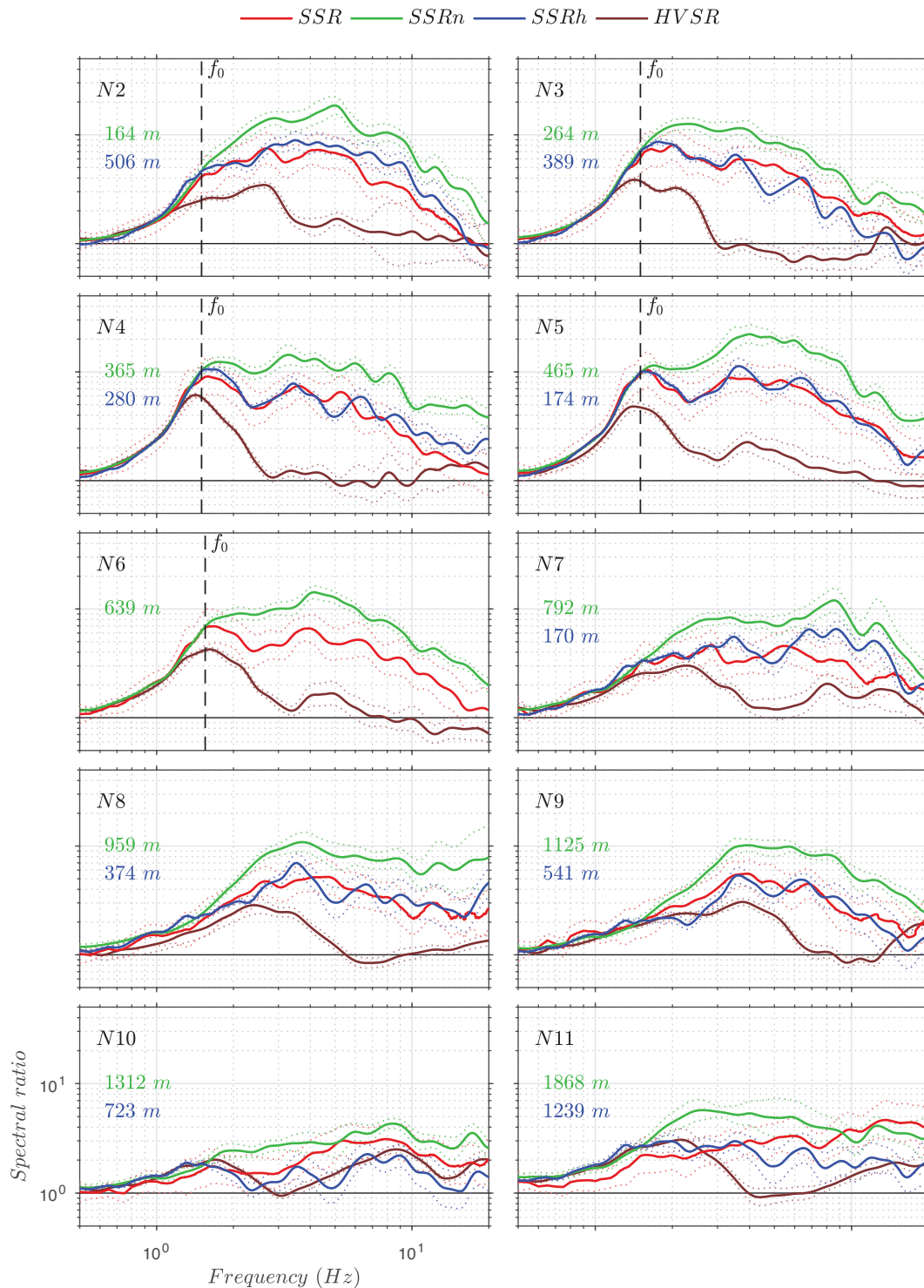


Figure 5. As for Fig. 4, but for stations N2–N11 in Argostoli, with the rock station N1 taken as reference, and N6 as the soil reference station used for the SSRh technique.

according to the possible presence of surface waves in the *S*-wave portion of the seismic signal that might be generated by near-site inhomogeneities. In the context of discussing comparisons between earthquake-based and noise-based results, Aki (1957) had already noted that, ‘it is well known that the characteristics of the ground

are reflected more or less in its vibration, whatever the origin of the vibration may be’. Our results appear to follow the same lines, especially in sedimentary basins where the strong trapping phenomena can result in seismic wavefields inside the basin that are strongly dominated by the basin response.

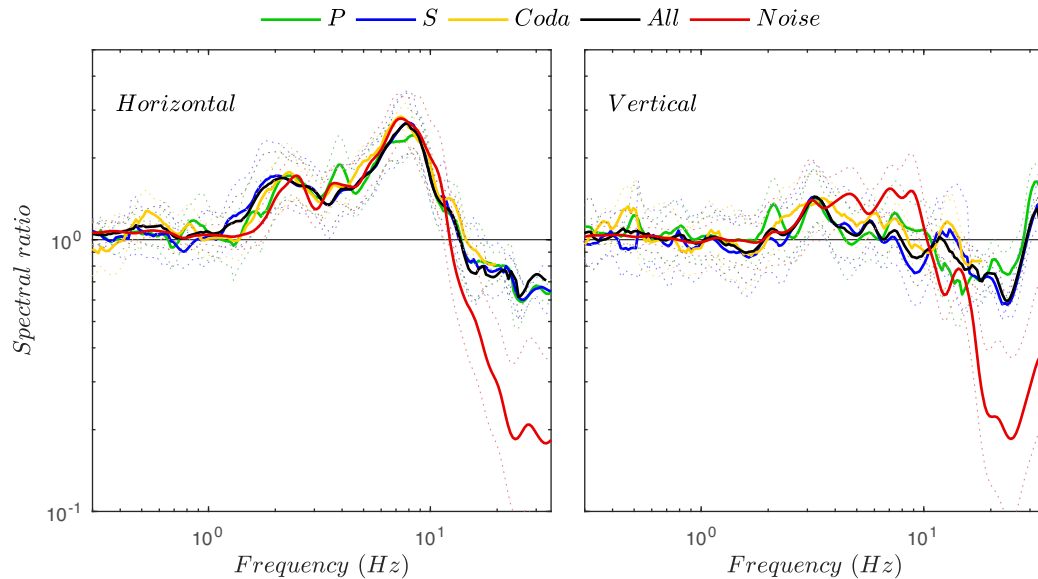


Figure 6. Comparisons of the SSRn (red) estimated from ambient noise between two stations located inside the basin in Provence (P3/P4) with the SSR estimated from various phases of the earthquake signal: Green, *P* waves; blue, *S* wave; yellow, coda waves; black, full signal. The horizontal mean and vertical components are represented in the left- and right-hand panels, respectively. The solid and dotted lines represent the geometric mean with its corresponding plus and minus standard deviation, computed from more than a hundred earthquakes for the SSR and from thousands of selected noise windows for the SSRn.

On the discrepancy between the rock-referenced SSRn and the SSR

Discrepancies between the SSRn and the SSR have been poorly discussed in the literature. The majority of the studies report an overestimation of the SSRn amplification factor referring to a rock site, especially at high frequency, but only a few studies investigated its origin. This over-amplification was often supposed to be due to the implantation of the rock reference site far from the human activities, in a quiet area, while the target soil sites are located inside the basin, where human activities are generally concentrated. The target soil site would thus be noisier than the reference rock site, which would induce a systematic overestimated ratio between the records from both sites. This interpretation cannot be supported in Argostoli, as the rock reference site is located in a noisier context to that of the basin station. Indeed, the rock reference station was located near to a road and the water pump factory of Argostoli, while most of the sedimentary stations were within Koutavos Park. Moreover, both the SSRn discrepancy and the SSRh similarity with respect to the SSR do not change much with the site-to-reference distance (from 87 to 1835 m). This supports the interpretation that our results are relatively insensitive to local noise source disturbance.

Here, we propose that the SSRn cannot assess the amplification at high frequency primarily because of the geological configuration. The physics of wave propagation state that the energy of the waves is partially trapped inside the sedimentary basin for frequencies greater than or equal to f_{0min} , due to the contrast of impedance between the soft sediments and the surrounding rock. If this phenomenon is known to explain part of the site effects, it also predicts that the basin represents a natural barrier for seismic waves, which limits their propagation into the stiffer medium surrounding the basin. Thereby, any rock site located near to the sedimentary basin might see only a limited part of the wave energy radiated at frequencies greater than f_{0min} if this energy is generated within the basin (or crosses the basin during its propagation). This might typically concern the ambient noise wavefield at the frequency range of interest, which is generated by local surface sources and propagates

at the Earth surface. In contrast, the body waves emitted by a distant earthquake are much less prone to such a phenomenon, as they are expected to arrive at the Earth surface with quasi-vertical incidence.

Nevertheless, the phenomenological difference between ambient noise and earthquake wavefields can explain at least a part of the discrepancy observed with the SSRn referring to the rock site when compared to the SSR. The rock-reference station records see, indeed, a truncated ambient noise wavefield for frequencies higher than f_{0min} , while this station is reached by the complete earthquake wavefield in the whole frequency band. This interpretation gives a suitable explanation for our observations: (i) the SSRn referring to the rock site beside the basin systematically overestimates (up to a factor 2–3) the amplification factor for frequencies higher than f_{0min} (e.g. SSRn above 4 Hz at sites P3 to P7 in Fig. 4, and above 1.5 Hz at sites N2 to N11 in Fig. 5). (ii) When both sites are inside the basin, the SSRn (here observed through the SSRh) provides a site transfer function which is similar to that obtained with the SSR in a broad frequency range (e.g. the SSRh at sites P3 to P7 in Fig. 4, N2 to N9 in Fig. 5, and direct SSRn at site P3 in Fig. 6). (iii) the observed SSRn discrepancy and the SSRh similarity to the SSR are independent of the site-to-reference distance.

Supporting this interpretation with numerical simulations will need to be done in the future. This might provide a physical interpretation in a controlled medium and promote the use of the SSRn inside sedimentary basins, with the aim to capture the spatial variability of the site response. Moreover, it could help to define the limits of this approach.

CONCLUSIONS

The use of ambient noise has received growing attention over almost a century, and more specifically since the 1980s for site effects purposes, with the introduction of the SSRn and the HVSR. Since then, increasing numbers of studies have focused on site effect analysis based on the HVSR, while the SSRn has been progressively abandoned. This can be explained by the success of the HVSR to assess

f_0 , while the SSRn amplification factors were generally unrealistically elevated at high frequencies (>1 Hz) where microtremors are dominated by human activities. Thus, retrieving the SSR transfer function from microtremors in a broad frequency range is very challenging, and to the best of our knowledge, this has never been successfully realized.

In this study, we compare the HVSR and the SSRn computed from microtremors with the classical SSR computed from earthquakes, for two different basins, the first in Provence (southeastern France) and the second in Argostoli (western Greece). In agreement with the literature, the HVSR only allow to recognize f_0 , as it does not provide the higher modes or the amplification factors. Moreover, it does not provide a reliable estimation of f_0 when 2-D or 3-D site effects induce broad-band amplifications. The SSRn shows similar site transfer functions when compared to the SSR for frequencies lower than the minimal fundamental resonance frequency of the basin (f_{0min}). For frequencies higher than f_{0min} , when the SSRn refers to the rock site located beside the basin, the amplification factors are widely overestimated (compared to the SSR). In contrast, when both stations are inside the basin, the SSRn is similar to the SSR in a broad frequency range (>10 Hz) for the two tested datasets. Based on these observations, we propose that the ambient noise wavefield generated inside and behind the basin (according to the rock reference site) is only partially transmitted to the rock reference site for frequencies higher than f_{0min} due to the contrast of impedance at the interface between the sediments and the rock. This effect is expected not to occur with distant earthquake body waves due to their quasi-vertical incidence at the basin and rock sites. This interpretation might explain why the rock-referring SSRn transfer functions overestimate the SSR amplification factor for frequencies higher than f_{0min} .

If this interpretation is correct, it might allow for new approaches that are based on ambient noise to estimate site effects. The SSRn might be a very practical and reliable tool to perform microzonation campaigns inside sedimentary basins, to provide then the relative site response at the scale of the entire basin and over a broad frequency range. The rock relative site response for the entire basin can then be deduced from information obtained at only one, or a few, site(s) inside the basin. In this respect, we introduce here the SSRh that aims to assess the spatial variability of the site response inside the basin from the SSRn, and then correct it by the rock relative SSR estimated at only one site inside the basin. This provides site transfer functions very comparable to the SSR up to high frequency (~12 Hz in Provence, ~20 Hz in Argostoli). This approach would be a very practical tool for broad-band microzonation inside sedimentary basins. However, this probably requires good knowledge of the geology beneath the area, and cross-validation with the SSR at a few sites inside the basin.

To conclude, we consider that the SSRn should receive renewed attention. Its physical understanding and further processing might benefit from the recent concepts developed in the framework of ambient noise correlations. Further investigations on the approaches and results presented here are necessary. Numerical modelling might be useful to more deeply understand the role of the basin on the ambient noise wavefield inside and outside the basin. Further research should also consider other sites, to understand to what extent and under which conditions these results might be applicable, and up to which frequency.

ACKNOWLEDGEMENTS

The authors are thankful to all of the participants of the Cashima, NERA and Sinaps@ projects for providing the Provence and Argostoli resources necessary for this study. Special thanks must go to Cédric Guyonnet-Benaize, Cécile Cornou, Elise Delavaud, Marc Nicolas, Olivier Sèbe, Bruno Hernandez, Afifa Imtiaz, Michel Campillo, Philippe Roux, Philippe Guéguen, Hiroshi Kawase, Emmanuel Chaljub and Christopher Berrie, for their comments or/and participation in this work. We are finally thankful to Behzad Hassani and an anonymous reviewer for their constructive reviews.

REFERENCES

- Aki, K., 1988. Local site effects on ground motion, *Earthq. Eng. Soil. Dyn. II-Recent Adv. Ground Motion Eval. Geotech. Spec. Publ.*, **20**, 103–155.
- Aki, K., 1957. Space and time spectra of stationary stochastic waves, with special reference to microtremors, *Bull. Earthq. Res. Inst.*, **35**, 415–456.
- Atakan, K., 1997. Empirical site response studies in Central America: present status, in *Proceedings, Seminar on Evaluation and Mitigation of Seismic Risk in the Central American Area, Universidad Centroamericana "Jose Simeón Cañas, San Salvador, El Salvador*, pp. 22–26.
- Baig, A.M., Campillo, M. & Brenguier, F., 2009. Denoising seismic noise cross correlations, *J. geophys. Res.: Solid Earth*, **114**, B08310.
- Bard, P.-Y., 1999. Microtremor measurements: a tool for site effect estimation?, in *Proceedings of the 2th IASPEI/IAEE (ESG2)*, Yokohama, Japan, 1998 December 1–3, pp. 1251–1279.
- Bensen, G.D., Ritzwoller, M.H., Barmin, M.P., Levshin, A.L., Lin, F., Moschetti, M.P., Shapiro, N.M. & Yang, Y. 2007. Processing seismic ambient noise data to obtain reliable broad-band surface wave dispersion measurements, *Geophys. J. Int.*, **169**, 1239–1260.
- Bonilla, L.F., Steidl, J.H., Lindley, G.T., Tumarkin, A.G. & Archuleta, R.J., 1997. Site amplification in the San Fernando Valley, California: variability of site-effect estimation using the S-wave, coda, and H/V methods, *Bull. seism. Soc. Am.*, **87**, 710–730.
- Bonnefoy-Claudet, S., Cornou, C., Bard, P.-Y., Cotton, F., Moczo, P., Kristek, J. & Fäh, D., 2006a. H/V ratio: a tool for site effects evaluation. Results from 1-D noise simulations, *Geophys. J. Int.*, **167**, 827–837.
- Bonnefoy-Claudet, S., Cotton, F. & Bard, P.-Y., 2006b. The nature of noise wavefield and its applications for site effects studies, *Earth Sci. Rev.*, **79**, 205–227.
- Borcherdt, R.D., 1970. Effects of local geology on ground motion near San Francisco Bay, *Bull. seism. Soc. Am.*, **60**, 29–61.
- Bowden, D.C., Tsai, V.C. & Lin, F.C., 2015. Site amplification, attenuation, and scattering from noise correlation amplitudes across a dense array in Long Beach, CA, *Geophys. Res. Lett.*, **42**, 1360–1367.
- Burjánek, J., Moore, J.R., Yügsi Molina, F.X. & Fäh, D., 2012. Instrumental evidence of normal mode rock slope vibration: evidence of normal mode rock slope vibration, *Geophys. J. Int.*, **188**, 559–569.
- Celebi, M., Dietel, C., Prince, J., Onate, M. & Chavez, G., 1987. Site amplification in Mexico City (determined from 19 September 1985 strong-motion records and from recordings of weak motions), *Dev. Geotech. Eng.*, **44**, 141–151.
- Cultrera, G., De Rubeis, V., Theodoulidis, N., Cadet, H. & Bard, P.-Y., 2014. Statistical correlation of earthquake and ambient noise spectral ratios, *Bull. Earthq. Eng.*, **12**(4), 1493–1514.
- Cushing, E.M. et al., 2016. Close to the lair of Odysseus Cyclops: the SINAPS@ postseismic campaign and accelerometric network installation on Kefalonia island – Site effect characterization experiment, in *Proceedings of the 7th International INQUA Meeting on Paleoseismology*, Crestone, CO, USA, 2016 May 30–June 3.

- Denolle, M.A., Dunham, E.M., Prieto, G.A. & Beroza, G.C., 2013. Ground motion prediction of realistic earthquake sources using the ambient seismic field, *J. geophys. Res.: Solid Earth*, **118**, 2102–2118.
- Dravinski, M., Ding, G. & Wen, K.-L., 1996. Analysis of spectral ratios for estimating ground motion in deep basins, *Bull. seism. Soc. Am.*, **86**, 646–654.
- Ferritto, J., 1995. *Ground Motion Amplification Using Microseisms*, in Int. Conf. Recent. Adv. Geotech. Earthq. Eng. Soil. Dyn., St. Louis, Missouri, 561–566, 1995 April 2–7.
- Ferritto, J.M., 1996. Repeatability of microseism measurements in Port Hueneme case study, *Bull. seism. Soc. Am.*, **86**, 428–435.
- Field, E.H., 1996. Spectral amplification in a sediment-filled valley exhibiting clear basin-edge-induced waves, *Bull. seism. Soc. Am.*, **86**, 991–1005.
- Field, E.H. *et al.*, 1995. Earthquake site-response study in Giumri (formerly Leninakan), Armenia, using ambient noise observations, *Bull. seism. Soc. Am.*, **85**(1), 349–353.
- Field, E.H., Hough, S.E. & Jacob, K.H., 1990. Using microtremors to assess potential earthquake site response: a case study in Flushing Meadows, New York City, *Bull. seism. Soc. Am.*, **80**, 1456–1480.
- Field, E.H. & Jacob, K.H., 1995. A comparison and test of various site-response estimation techniques, including three that are not reference-site dependent, *Bull. seism. Soc. Am.*, **85**, 1127–1143.
- Field, E.H. & Jacob, K.H., 1993. The theoretical response of sedimentary layers to ambient seismic noise, *Geophys. Res. Lett.*, **20**, 2925–2928.
- Garofalo, F. *et al.*, 2016. InterPACIFIC project: comparison of invasive and non-invasive methods for seismic site characterization. Part II: inter-comparison between surface-wave and borehole methods, *Soil. Dyn. Earthq. Eng.*, **82**, 241–254.
- Gaull, B.A., Kagami, H. & Taniguchi, H., 1995. The microzonation of perth, Western Australia, using microtremor spectral ratios, *Earthq. Spectra*, **11**, 173–191.
- Gitterman, Y., Zaslavsky, Y., Shapira, A. & Shtivelman, V., 1996. Empirical site response evaluations: case studies in Israel, *Soil. Dyn. Earthq. Eng.*, **15**, 447–463.
- Gutierrez, C. & Singh, S.K., 1992. A site effect study in Acapulco, Guerrero, Mexico: comparison of results from strong-motion and microtremor data, *Bull. seism. Soc. Am.*, **82**, 642–659.
- Haile, M., Seo, K., Kurita, K. & Nakamaru, A., 1997. Study of site effects in kobe area using Microtremors, *J. Phys. Earth*, **45**, 121–133.
- Hashemi, H. & Maazallahi, M., 2012. Comparison of SSR and H/V microtremor data analysis techniques, *J. Earth Space Phys.*, **38**, 85–92.
- Hollender, F. *et al.*, 2015. Close to the lair of Odysseus Cyclops: the SINAPS@ post-seismic campaign and accelerometric network installation on Kefalonia Island, in *Proceedings of the 9ème Colloque National AFPS*, Marne-la-Vallée, France 2015 November 30–December 2.
- Horiike, M., Zhao, B. & Kawase, H., 2001. Comparison of site response characteristics inferred from microtremors and earthquake shear waves, *Bull. seism. Soc. Am.*, **91**, 1526–1536.
- Ibs-von Seht, M. & Wohlenberg, J., 1999. Microtremor measurements used to map thickness of soft sediments, *Bull. seism. Soc. Am.*, **89**, 250–259.
- Imtiaz, A., Perron, V., Svay, A., Hollender, F., Bard, P.-Y. & Theodoulidis, N., 2017. Wavefield characteristics and coherency of seismic ground motion from a rock site at Argostoli, Greece, in *Proceedings of the 16th World Conference on Earthquake Engineering (16WCEE)*, Santiago, Chile, 2017 January 9–13.
- Irikura, K. & Kawanaka, T., 1980. Characteristics of microtremors on ground with discontinuous underground structure, *Bull. Disas Prev Res Inst.*, **30**, 81–96.
- Ishimoto, M., 1937. Observations sur des secousses d'une petite amplitude, *Bull. Earthq. Res. Inst.*, **15**, 697–705.
- Kagami, H., Duke, C.M., Liang, G.C. & Ohta, Y., 1982. Observation of 1-to 5-second microtremors and their application to earthquake engineering. Part II. Evaluation of site effect upon seismic wave amplification due to extremely deep soil deposits, *Bull. seism. Soc. Am.*, **72**, 987–998.
- Kagami, H., Okada, S., Shiono, K., Oner, M., Dravinski, M. & Mal, A.K., 1986. Observation of 1-to 5-second microtremors and their application to earthquake engineering. Part III. A two-dimensional study of site effects in the San Fernando Valley, *Bull. seism. Soc. Am.*, **76**, 1801–1812.
- Kawase, H., Matsushima, S., Satoh, T. & Sánchez-Sesma, F.J., 2015. Applicability of theoretical horizontal-to-vertical ratio of microtremors based on the diffuse field concept to previously observed data, *Bull. seism. Soc. Am.*
- Konno, K. & Ohmachi, T., 1998. Ground-motion characteristics estimated from spectral ratio between horizontal and vertical components of microtremor, *Bull. seism. Soc. Am.*, **88**, 228–241.
- Koyama, S., Okama, I., Kashima, T. & Kitagawa, Y., 1996. *Characteristics of Ground Motion in Kobé Area*, Acapulco, Mexico.
- Kudo, K., 1995. Practical estimates of site response. State-of-the-art report, in *Proceedings of the 5th International Conference on Seismic Zonation*, Nice, France, 1995 October 17–19.
- Lermo, J. & Chávez-García, F.J., 1994. Are microtremors useful in site response evaluation? *Bull. seism. Soc. Am.*, **84**, 1350–1364.
- Manchuel, K., Traversa, P., Baumont, D., Cara, M., Nayman, E. & Durouchoux, C., 2017. The French seismic CAtalogue (FCAT-17), *Bull. Earthq. Eng.*, 1–25.
- Melo, G., Malcolm, A., Mikesell, D. & van Wijk, K., 2013. Using SVD for improved interferometric Green's function retrieval, *Geophys. J. Int.*, **194**, 1596–1612.
- Milana, G., Barba, S., Pezzo, E.D. & Zambonelli, E., 1996. Site response from ambient noise measurements: new perspectives from an array study in Central Italy, *Bull. seism. Soc. Am.*, **86**, 320–328.
- Milne, J., 1908. *Seismology*, K. Paul, Trench, Trübner, 85.
- Nakamura, Y., 1989. A method for dynamic characteristics estimation of subsurface using microtremor on the ground surface, *Railw. Tech. Res. Inst. Q. Rep.*, **30**(1), 25–33.
- Nogoshi, M. & Igarashi, T., 1971. On the amplitude characteristics of microtremor (Part 2), *J. Seism. Soc. Jpn.*, **24**, 26–40.
- Ohmachi, T., Nakamura, Y. & Toshinawa, T., 1991. Ground motion characteristics of the San Francisco bay area detected by microtremor measurements, in *Int. Conf. Recent. Adv. Geotech. Earthq. Eng. Soil. Dyn.*, 1643–1648, St. Louis, Missouri, 1991 March 11–15.
- kada, S., Muraki, H.O. & Kagami, H., 1991. Two-dimensional analysis on site effects in the Sapporo Urban Region, Japan, based on observation of 1 to 10 second microtremors, in *Proceedings of the 4th International Conference on Seismic Zonation (4ICSZ)*, Stanford, CA, 1991 August 26–29.
- Perron, V., 2017. Apport des enregistrements de séismes et de bruit de fond pour l'évaluation site-spécifique de l'aléa sismique en zone de sismicité faible à modérée, *PhD thesis*, Université Grenoble Alpes.
- Perron, V., Hollender, F., Bard, P.-Y. & Hernandez, B., 2015. Site instrumentation usefulness: implementation recommendations and application examples of empirical site effect estimation in low to moderate seismicity context, in *Proceedings of the 9ème Colloque National AFPS*, Marne-la-Vallée, France, 2015 November 30–December 2.
- Perron, V., Hollender, F., Bard, P.-Y., Gélis, C., Guyonnet-Benaize, C., Hernandez, B. & Ktenidou, O., 2017a. Robustness of kappa (κ) measurement in low-to-moderate seismicity areas: insight from a site-specific study in Provence, France, *Bull. seism. Soc. Am.*, **107**, 2272–2292.
- Perron, V. *et al.*, 2018. Accelerometer, velocimeter Dense-Array, and rotation sensor datasets from the Sinaps@ Postseismic survey (Cephalonia 2014–2015 Aftershock Sequence), *Seismol Res Lett.*, **89**, 678–687.
- Perron, V., Laurendeau, A., Hollender, F., Bard, P.-Y., Gélis, C., Traversa, P. & Drouet, S., 2017b. Selecting time windows of seismic phases and noise for engineering seismology applications: a versatile methodology and algorithm, *Bull. Earthq. Eng.*, **16**(6), 2211–2225.
- Piña-Flores, J., Perton, M., García-Jerez, A., Carmona, E., Luzón, F., Molina-Villegas, J.C. & Sánchez-Sesma, F.J., 2017. The inversion of spectral ratio H/V in a layered system using the diffuse field assumption (DFA), *Geophys. J. Int.*, **208**, 577–588.
- Prieto, G.A., Denolle, M., Lawrence, J.F. & Beroza, G.C., 2011. On amplitude information carried by the ambient seismic field, *Comptes Rendus Geosci.*, **343**, 600–614.
- Roten, D., Fäh, D., Cornou, C. & Giardini, D., 2006. Two-dimensional resonances in Alpine valleys identified from ambient vibration wavefields, *Geophys. J. Int.*, **165**, 889–905.

- Rovelli, A., Singh, S.K., Malagnini, L., Amato, A. & Cocco, M., 1991. Feasibility of the use of microtremors in estimating site response During Earthquakes: some test cases in Italy, *Earthq Spectra*, **7**, 551–561.
- Sánchez-Sesma, F.J. *et al.*, 2011. A theory for microtremor H/V spectral ratio: application for a layered medium, *Geophys. J. Int.*, **186**, 221–225.
- Satoh, T., Kawase, H. & Matsushima, S., 2001. Differences between site characteristics obtained from microtremors, S-waves, P-waves, and codas, *Bull. seism. Soc. Am.*, **91**, 313–334.
- Seats, K.J., Lawrence, J.F. & Prieto, G.A., 2012. Improved ambient noise correlation functions using Welch's method, *Geophys. J. Int.*, **188**, 513–523.
- Seekins, L.C., Wennerberg, L., Margheriti, L. & Liu, H.-P., 1996. Site amplification at five locations in San Francisco, California: a comparison of S waves, codas, and microtremors, *Bull. seism. Soc. Am.*, **86**, 627–635.
- Seo, K., 1992. A joint work for measurements of microtremors in the Ashigara valley, in *Proceedings of the 1st IASPEI/IAEE (ESG1)*, Odawara, Japan, 1992 March 25–27, pp. 43–52.
- Seo, K. *et al.*, 2000. A joint research on microtremors in Fukui basin, Japan—For site effects evaluation during the 1948 Fukui (Japan) Earthquake, in *Proceedings of the onference on Earthquake Engineering (12WCEE)*, Auckland, New Zealand, 2000 January 30–February 4.
- SESAME team, 2004. Guidelines for the implementation of the H/V spectral ratio technique on ambient vibrations: measurements, processing and interpretation, SESAME European research project.
- Steimen, S., Fäh, D., Kind, F., Schmid, C. & Giardini, D., 2003. Identifying 2D resonance in microtremor wave fields, *Bull. seism. Soc. Am.*, **93**, 583–599.
- Theodoulidis, N., 2006. Site characterization using strong motion and ambient noise data: Euroseistest (N. Greece), in *Proceedings of the 3th IASPEI/IAEE (ESG3)*, Grenoble, France, 2006 August 30–September 1, pp. 1–10.
- Theodoulidis, N. *et al.*, 2018. Basin effects on ground motion: the case of a high-resolution experiment in Cephalonia (Greece), *Bull Earthq Eng*, **16**(2), 529–560.
- Yamanaka, H., Dravinski, M. & Kagami, H., 1993. Continuous measurements of microtremors on sediments and basement in Los Angeles, California, *Bull. seism. Soc. Am.*, **83**, 1595–1609.
- Yoritomo, J.Y. & Weaver, R.L., 2016. Fluctuations in the cross-correlation for fields lacking full diffusivity: the statistics of spurious features, *J. acoust. Soc. Am.*, **140**, 702–713.
- Zhao, B.M., Horike, M. & Takeuchi, Y., 1998. Reliability of estimation of seismic ground characteristic by microtremor observation, in *Proceedings of the 11th European Conference on Earthquake Engineering (11ECEE)*, Paris, France, 1998 September 6–11, pp. 6–11.